ICAS 2016
30th Congress of the International Council of the Aeronautical Sciences
DCC, Daejeon, Korea ; September 25-30, 2016

CHARACTERIZATION OF THE NONLINEAR AEROELASTIC BEHAVIOR OF AN AIRFOIL WITH FREEPLAY AND AERODYNAMIC NONLINEARITY

Michael Candon, Robert Carrese, Hideaki Ogawa, Pier Marzocca
School of Engineering (Aerospace Engineering and Aviation)
RMIT University

Keywords: *nonlinear aeroelasticity, freeplay, aerodynamic nonlinearity, higher-order spectra, system identification*

Abstract

Higher-order spectra (HOS) are utilized to investigate the nonlinear flutter behavior of a two-dimensional pitch/plunge airfoil system in transonic flow with freeplay and aerodynamic nonlinearity. It is shown that on the route to diverging flutter the system begins with the pitching and plunging modes being uncoupled and undergoes various evolutions exhibiting quasi-periodic behavior as it moves towards an ordered state of high-amplitude periodic limit cycle behavior. New physical insights come from the bispectral densities being computed at critical stages as the system evolves from through different stages of periodicity with the coalescence of the pitching and plunging frequencies into a single coupled limit cycle. Based on these estimates the nonlinear interaction mechanisms which occur within the nonlinear aeroelastic system prior to diverging flutter can be characterized. Furthermore, aerodynamic nonlinearity in the form of Tijdeman Type-B shock motion is quantified and its effect in combination with freeplay assessed.

1 Introduction

Understanding the effect of nonlinearity on the aeroelastic response of two- and three-dimensional aeroelastic systems is currently a crucial and active field of research, driven by the undesirable and sometimes dangerous effects that nonlinear aeroelastic phenomena can have on a systems structural health. Within the body of knowledge surrounding aeroelasticity for aircraft it is well documented in the literature that both aerodynamic and structural nonlinearity can induce undesirable nonlinear aeroelastic phenomena compromising the structural integrity of airframes. Most commonly limit cycle oscillation (LCO) is observed and is characterized by high-amplitude sustained dynamic wing oscillations. Furthermore, it has been well documented that within particular regions of the flight envelope, the dynamic LCO behavior can undergo various bifurcations and even exhibit aperiodic or chaotic tendencies. Aerodynamic nonlinearity is generally a result of transonic flow phenomena, *i.e.*, shock wave-boundary layer interactions and shock induced separation, high angle of attack dynamic stall operations or, within critical regions of the flight regime, the resulting transonic buffet. Structural nonlinearity can be either distributed or concentrated. A distributed nonlinearity will affect the entire wing (*i.e.*, nonlinear material properties or geometrical due to large amplitude), whereas concentrated nonlinearity is the result of large concentrated structural loads or freeplay [1]. Current design criteria with respect to aeroelasticity are outdated and conservative, often based on linear models and an elementary comprehension of nonlinear aeroelastic phenomena. Hence, it is necessary to improve our understanding of nonlinear aeroelastic phenomena allowing for less conservative design criteria to be established for aeroelastic design and certification.

The nonlinear aeroelastic phenomena mentioned here have been studied rigorously for two-dimensional airfoil systems in subsonic flow regimes with freeplay nonlinearity. More specifically, considerable progress was made for two-degree-of-freedom (2-DOF) systems (*i.e.*, excluding a control surface) two-decades ago [2] and recently revisited [3, 4]. It has been shown that nonlinearity induces LCO well

below the linear flutter boundary, that as the flight speed increases the system can exhibit chaotic tendencies and on the route to chaos various bifurcations occur. Further, the sensitivity of these phenomena to various aerodynamic and structural parameters is presented. Studies to this effect have also been conducted (less frequently) for transonic/ supersonic flow regimes, authoritative examples are given in [5, 6]. In particular within transonic/low supersonic flow regimes research of this nature is scarce, hampered by the difficulties associated with modeling transonic flow. The studies mentioned here couple the nonlinear structural equations of motion with aerodynamic models of varying fidelity, this ranges from transient computational fluid dynamics (CFD) simulations to simplified analytical equations.

Higher-order spectra (HOS) analysis is a valuable tool when analyzing nonlinear aeroelastic systems. The superiority of HOS when comparing to traditional linear methods, such as the power spectrum, comes from the ability of the higher-order statistics to predict the presence of nonlinearity. The power spectrum is only able to define second-order statistics, therefore, can only rigorously unveil physics associated with linear phenomena [7]. HOS methods are advantageous in nonlinear aeroelastic analysis as they demonstrate interactions between frequencies which are a result of nonlinearity, hence, HOS can be used to identify the presence of nonlinearity and the transition from linear to nonlinear behaviour within an aeroelastic system. It is also worth noting the duality between HOS and Volterra functional series' kernels, where HOS can be represented as the Fourier transform of the Volterra series, *i.e.*, the Volterra series in the frequency-domain.

HOS analysis has been applied recently to flight test, wind tunnel and numerical data to investigate the nonlinear aeroelastic aspects of various full aircraft, wing and airfoil configurations. It is shown that HOS analysis is able to detect the presence of nonlinearity, provide insight into the transition from linear to nonlinear behavior, indicate regions in which the nonlinear source is located, identify nonlinear interactions between a systems various frequency components and provide insight into how parametric variation affects the nonlinear interaction of frequency components [8 – 14].

Although significant progress has been made in understanding the limit cycle, bifurcation and chaotic tendencies of two-dimensional airfoil systems with freeplay, the underlying nonlinear frequency interactions which occur as a result of these phenomena is yet to be considered. Hence an extended approach to the traditional analysis methods for bifurcating systems is presented. HOS analysis is used to provide novel insights into how the systems frequency components couple nonlinearly as the system evolves from aperiodic dynamic response to LCO and diverging flutter and, in the process aerodynamic nonlinearity becomes prevalent.

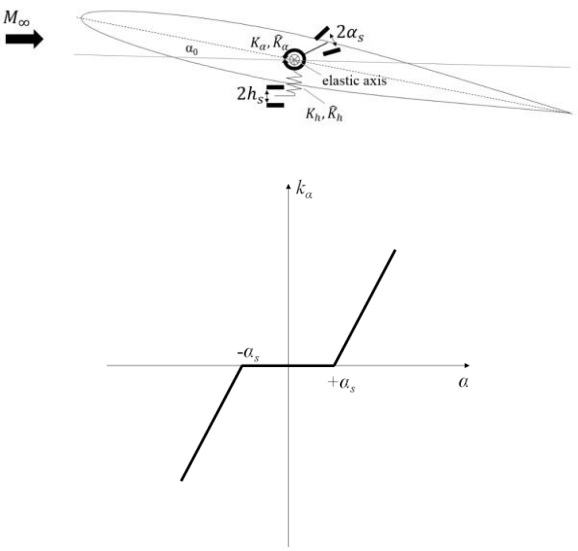

Figure 1: NACA 64A010 pitch/plunge airfoil system with concentrated structural nonlinearity (top) and pitching freeplay stiffness nonlinearity (bottom)

In the present study HOS are used to analyze the nonlinear frequency interactions which occur within a two-dimensional pitch / plunge airfoil system in transonic flow with pitching freeplay nonlinearity. Various reduced velocities are investigated with the bispectral densities being computed at various critical stages pre-diverging flutter. The results are presented in the form of phase-plane plots,

pressure coefficient distributions and bicoherence contours. The Isogai benchmark aeroelastic system [15] is considered modified to include the structural nonlinearity (Fig. 1). The system is represented by coupling a high-fidelity computational fluid dynamics (CFD) solver for the viscous compressible flow-fields with the nonlinear equations of motion for the pitch / plunge system. This approach to analyzing nonlinear aeroelastic configurations provides valuable insights into the underlying frequency content of the nonlinear system and the methodology seeds the development of an online system identification framework for aircraft.

2 Computational Framework

In this study, two-way fluid-structure interaction (FSI) simulations are performed; this sophisticated numerical technique couples the transient rigid body pitch/plunge airfoil motion with high-fidelity Euler-CFD to solve for the compressible transient flow-fields.

2.1 Conditions and Configuration

The present study considers fixed structural parameters with an incremental increase in the reduced velocity U^* where $U^* = U_\infty/b\omega_\alpha$ and U_∞ is the freestream velocity, b is the semi-chord and ω_α is the frequency of the torsional mode. U^*_f represents the reduced velocity at the linear flutter boundary (no freeplay). The freestream Mach number remains fixed at M = 0.8 whilst the remainder of the freestream variables vary to account for the varying freestream reduced velocity value.

A benchmark case often used for numerical comparison is the Isogai Case A, a two-dimensional pitch / plunge aeroelastic model with a NACA 64A010 airfoil section [15]. The flutter boundary at zero mean angle of attack is a highly investigated numerical benchmark for methods predicting aeroelastic instabilities in the literature. The dimensionless structural parameters of this configuration are chosen to represent the dynamics of the outer section of a swept-back wing, with center-of-gravity, x_{CG} = 0.4, with offset to center-of-rotation, x_α = -1.8, and radius-of-gyration about the center-of-rotation, r_α = 1.865. This places the pivot point forward of the leading edge. The ratio of natural (uncoupled) frequencies $\bar{\omega} = \omega_h/\omega_\alpha$ = 0.7, and a mass ratio μ = 60. The dimensionless chord length $2b$ is 1. No structural damping is considered. For validation of the aeroelastic case, see reference [13]. The structural parameters of the Isogai case are modified in the interest of the present study and to account for the concentrated structural nonlinearity. The remaining structural parameters are summarized in Table 1.

Table 1: Structural parameters per unit span

m (kg per unit chord)	10
I_α (kg·(unit chord)^2)	17.4
S_α (kg·(unit chord)^2/s^2)	9
α_0 (°)	0
α_s (°)	0.5
ω_h (Hz)	9.42
ω_α (Hz)	13.49
$\bar{\omega}$	0.7

2.2 Computational Fluid Dynamics

The Euler equations for transient flow-fields are solved via a coupled pressure-based solver with second order upwind spatial accuracy. The convergence criteria are set to 1e-03 for the scaled residuals at each time step. In order to facilitate the movement of the airfoil, the C-type grid (Fig. 2) is designed in the interest of preserving cell quality. The grid consists of approximately 9000 cells. A dynamic mesh with a smoothing method is utilized. The smoothing method allows the interior nodes of the mesh to deform whilst the number of nodes and their connectivity remain preserved. In order to facilitate the movement of the wing, a dynamic mesh with a smoothing method is utilized. The smoothing method allows the interior nodes of the mesh to deform whilst the number of nodes and their connectivity remain preserved. A diffusion smoothing method is implemented with a diffusion parameter of 1.5 aiming to preserve cells closest to the wall and apply the dynamic motion to the cells in the interior of the far-field. The diffusion smoothing method is chosen as it generally results in a better quality

mesh when compared to other smoothing methods such as spring-based smoothing [16].

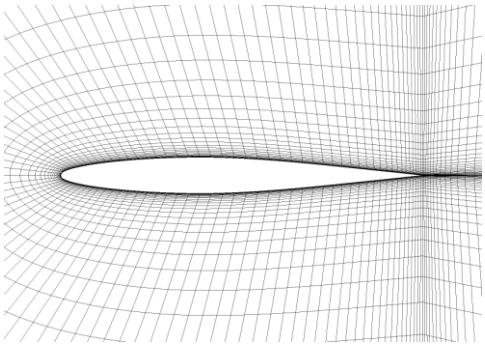

Figure 2: Computational grid

2.3 Structural Solver

In the present paper the Isogai Case A two-dimensional pitch / plunge aeroelastic system [15] is modified to account concentrated structural nonlinearity, introduced via a pitching freeplay dead-zone α_s. The freeplay nonlinearity is effectively a discontinuity within the aeroelastic system whereby for $-\alpha_s \leq \alpha \leq \alpha_s$ the torsional stiffness is zero.

The nonlinear governing equations are derived from the Lagrange equations, from small angle approximation

$$m\ddot{h} + S_\alpha \ddot{\alpha} + c_h \dot{h} + F(h) = L(t) \qquad (1)$$

$$S_\alpha \ddot{h} + I_\alpha \ddot{\alpha} + c_\alpha \dot{\alpha} + G(\alpha) = M_{EA}(t) \qquad (2)$$

where h represents plunging motion and α represents pitching motion and, $F(h), G(\alpha)$ are the nonlinear stiffness and c_h, c_α and damping coefficients, respectively. In addition, S_α is the static unbalance moment about the elastic axis per unit chord and I_α is the cross-section mass moment of inertia about the elastic axis per unit chord. L is the time varying lift per unit chord and M_{EA} is the time varying aerodynamic moment about the elastic axis per unit chord. $F(h)$ and $G(\alpha)$ can be defined by

$$F_a(h) = K_h h \qquad (3)$$

$$G_a(\alpha) = K_\alpha \alpha \text{ for } \alpha > \alpha_s; \quad 0 \text{ for } -\alpha_s \leq \alpha \leq \alpha_s; \quad K_\alpha \alpha \text{ for } \alpha < -\alpha_s \qquad (4)$$

The nonlinear governing equations can be represented in matrix form as

$$\begin{bmatrix} m & S_\alpha \\ S_\alpha & I_\alpha \end{bmatrix} \begin{bmatrix} \ddot{h} \\ \ddot{\alpha} \end{bmatrix} + \begin{bmatrix} F_a & 0 \\ 0 & G_a \end{bmatrix} = \begin{bmatrix} L(t) \\ M_{EA}(t) \end{bmatrix} \qquad (5)$$

Finally this can be represented by a system of first-order equations and solved via the fourth-order Runge-Kutta scheme.

2.4 Fluid Structure Interaction

The FSI simulations are computed using the commercial CFD solver ANSYS Fluent 16.2 [16]. The nonlinear pitch/plunge structural system is embedded within the ANSYS Fluent solver via a user defined function (UDF). Explicit coupling between the aerodynamic and structural models are achieved via UDF to prescribe generalized motion of the airfoil. The value of the dynamic time step must be low enough to capture the motion of the airfoil within the discontinuous freeplay zone; Δt = 0.001 s is considered sufficient. The transient simulations are initialized from a converged steady-state solution.

2.5 Higher-Order Spectra

Bispectral density or bispectrum can be used to identify nonlinear aspects within the aeroelastic system, *i.e.*, more specifically concentrated structural or aerodynamic nonlinearity. The bispectrum determines nonlinear interactions within the aeroelastic system by estimating third-order moments in the frequency-domain [7]. The bispectral density is defined as

$$B(f_1, f_2) = \frac{1}{M} \sum_{i=1}^{M} X_i(f_1) X_i(f_2) X_i^*(f_1 + f_2) \qquad (6)$$

where M is the number of data segments to be considered. The bispectrum $B(f)$ can be plotted against two frequency variables f_1 and f_2 in a three-dimensional plot. Each point on the plot describes the bispectral energy density of the signal at the bifrequency (f_1, f_2). The bispectrum at any bifrequency (f_1, f_2) measures the level of interaction between the two frequencies f_1 and f_2, which is the result of a quadratic phase relationship being present between them; hence

the bispectrum detects the presence of quadratic nonlinearity. *X(f)* is the Fourier transform of the time series *x(t)* [7].

Whilst the bispectrum detects system quadratic nonlinearity, it does not provide a basis for comparing levels of nonlinearity, hence, as a general practice; the bispectrum is conveniently normalized to give the bicoherence which is bounded between 0 and 1, where spikes in the magnitude of the bicoherence function represent levels nonlinearity.

The bicoherence function b can be defined as

$$b(f_1, f_2) = \frac{\left|\frac{1}{M}\sum_{i=1}^{M} X_i(f_1)X_i(f_2)X_i^*(f_1+f_2)\right|^2}{\frac{1}{M}\sum_{i=1}^{M}|X_i(f_1)X_i(f_2)|^2 \cdot \frac{1}{M}\sum_{i=1}^{M}|X_i(f_1+f_2)|^2} \quad (7)$$

In estimating the higher-order spectra, the data is split into blocks which are evaluated individually and averaged. It is essential that particular attention be given to the block length M in comparison to the total data length N. A larger the block size will provide a finer resolution, but this comes with greater variance [17]. It is suggested by Dalle Molle and Hinch [18] that when identifying n^{th}-order cumulants, the block length should be $(n-1)^{th}$ root of the sample size. To estimate the bispectrum (bicoherence) numerical codes are implemented based on validation provided in a previous study with multiple degrees of freedom mechanical systems [19]. The mechanical system is presented in Reference [20], providing the reader with an example to support the use of HOS and understand its features. In the present research N = 32,768 data points are used with a block length of M = 1024 (1024-point FFT).

3 Results

The results of the analysis are presented in the form phase plane plots, pressure coefficient distributions and bicoherence contours.

Figures 3 and 4 present the phase-plane diagrams for the system at U^* = 0.3, 0.4, 0.5, 0.7 and 0.73. The linear flutter boundary is found to be at $U^* = U^*_f$ = 0.74. It can be seen that U^* = 0.3 the motion is characterized by aperiodicity and low amplitude oscillations. As the velocity index is increased to U^* = 0.4 and 0.5 the system moves to a more ordered state, however, the pitching and plunging amplitudes do not increase significantly. At U^* = 0.7 typical limit cycle behavior is observed and the amplitude of the oscillations increases significantly. Finally at U^* = 0.73 (just below the linear flutter boundary) the amplitude of the oscillations increases again and the peaks (although in LCO) appear scattered about a constant minima/ maxima.

To give insight into the presence of aerodynamic nonlinearity the pressure coefficients on the upper and lower airfoil surface are displayed in Figures 5 – 8. It can be seen that at U^* = 0.3 the shift of the shock position and strength is insignificant. Furthermore, at this condition aerodynamic effects are minimal (considering the definition of the reduced velocity). This means that shock motion at this condition has negligible effect on the system. At U^* = 0.5 the strength and position of the shock have a greater variance, although still appears to be linear (*i.e.* the shock motion sinusoidal and linearly/weakly nonlinearly proportional to the structure). At U^* = 0.7 it can be seen that the strength and position of the shock varies significantly and, at particular stages of the cycle, ceases to exist on one surface whilst being strong on the opposing surface. Thus the aerodynamic nonlinearity is considered to be Tijdeman Type-B shock motion. Finally, the strength of the nonlinear aerodynamics can be seen to increase again at U^* = 0.73.

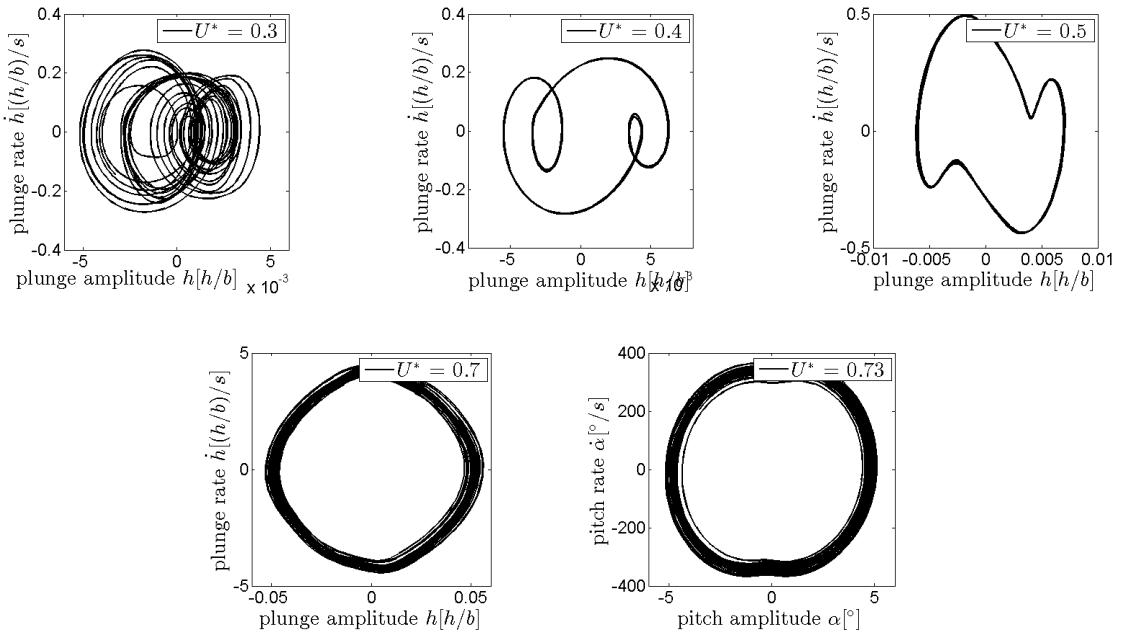

Figure 3: Phase plane diagrams for the plunge DOF

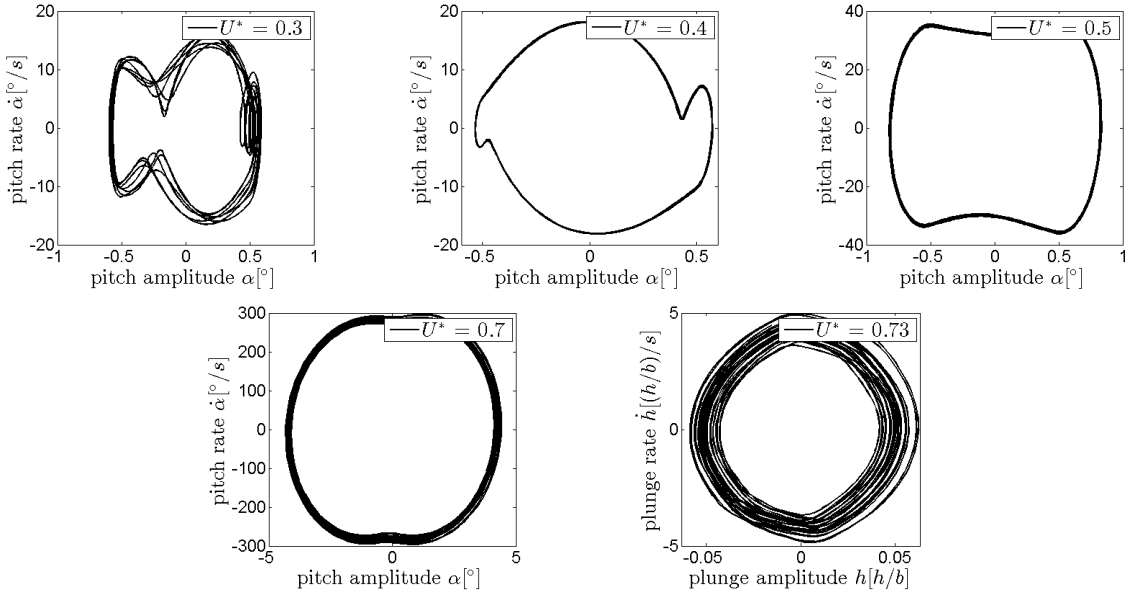

Figure 4: Phase plane diagrams for the pitch DOF

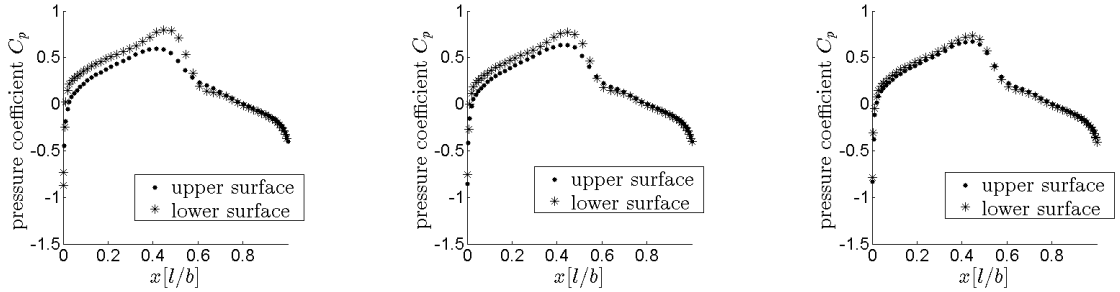

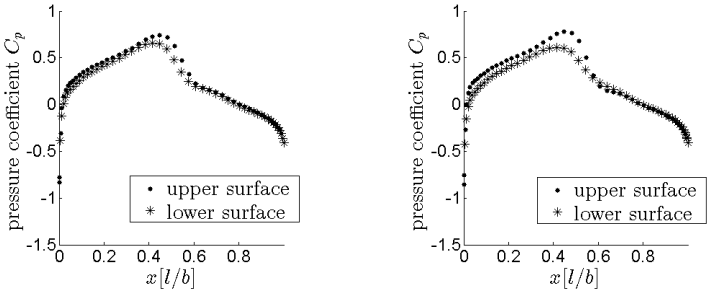

Figure 5: Pressure coefficient distributions for half of one cycle at *U = 0.3**

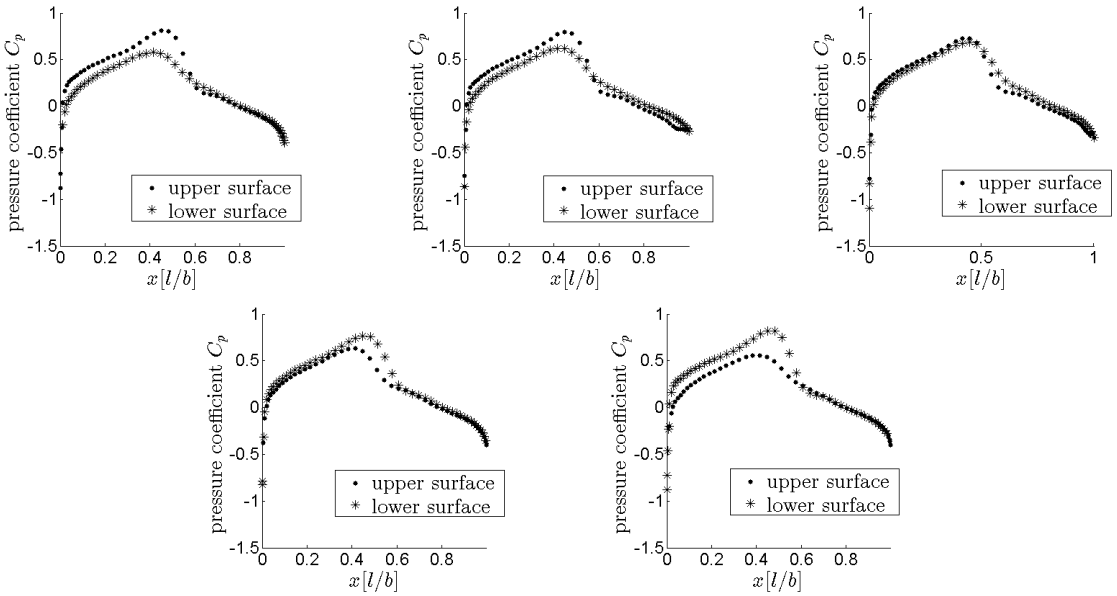

Figure 6: Pressure coefficient distributions for half of one cycle at *U = 0.5**

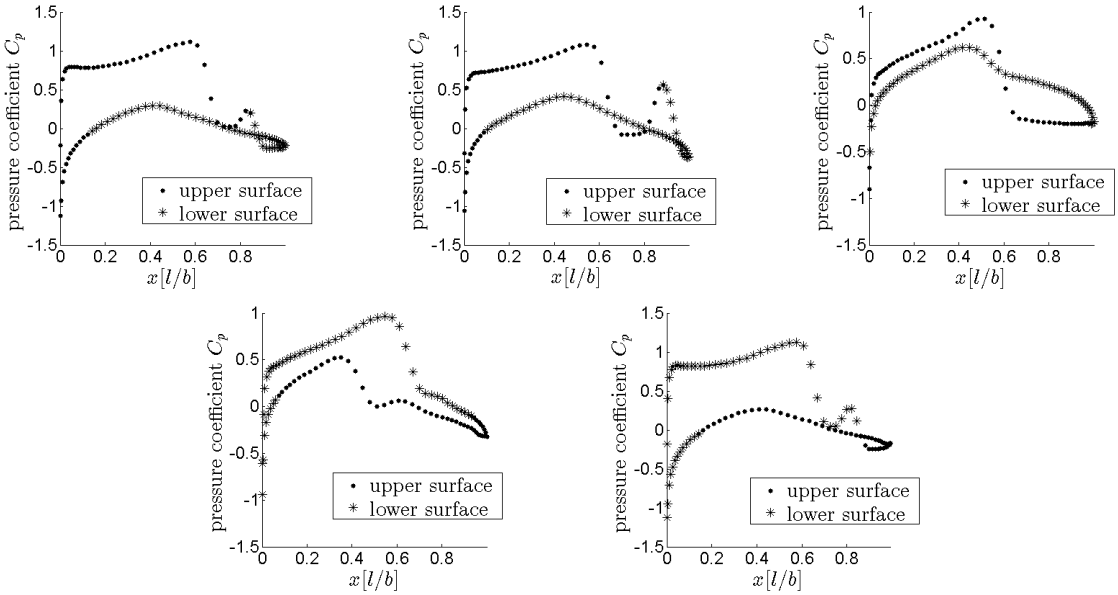

Figure 7: Pressure coefficient distributions for half of one cycle at *U = 0.7**

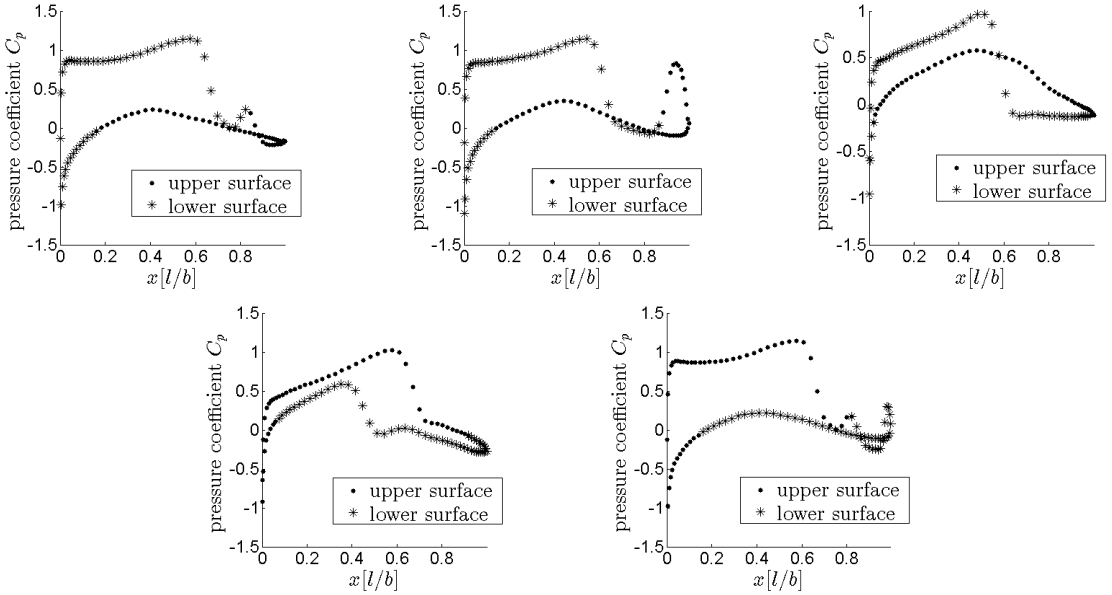

Figure 8: Pressure coefficient distributions for half of one cycle at $U^* = 0.73$

To gain further insight into the behavior of the system as the oscillations shift from aperiodic to limit cycle the bicoherence is estimated as presented in Figures 9 and10. This provides insight into the frequency content of the system and the quadratic interactions which occur between frequency components. It is identified that at $U^* = 0.3$ the frequency of the pitching DOF f_α is 3.5 Hz and is driven by the freeplay and aerodynamic loading (lack thereof) on the system. Furthermore, the impact between the airfoil and the pitching freeplay constraint activates the natural bending mode (ω_h = 9.42 Hz) which drives the dynamic plunging oscillations f_h. Here in the plunging mode a strong quadratic interaction is observed where f_α couples with f_h. Furthermore, there is also a moderate interaction via the self-interaction of ($f_\alpha + f_h$). Weak interactions are observed via the self-interaction of f_α and where f_h couples with $f_\alpha + f_h$. In pitch there is a strong quadratic coupling via the self-interaction of f_α and weak coupling via the interactions already mentioned.

It can be seen that at $U^* = 0.4$ the natural bending mode has decoupled and the frequency of the plunging DOF shifts to the pitching frequency superharmonic $f_h = 3f_\alpha$. The bicoherence now exhibits well-defined peaks where the pitching frequency f_α and its three superharmonics ($2f_\alpha$, $3f_\alpha$, $4f_\alpha$) are all involved in various nonlinear interactions. In plunge there is strong quadratic coupling where f_α interacts with $3f_\alpha$ and moderate quadratic coupling via the self-interaction of $3f_\alpha$. In pitch there is strong quadratic coupling via the self-interaction of f_α and moderate quadratic coupling where f_α interacts with $3f_\alpha$. At $U^* = 0.5$ the frequencies of the pitching and plunging oscillations have coalesced to f_α which is in the vicinity of the first natural bending frequency. The interaction between f_α and $2f_\alpha$ is of moderate magnitude in the plunging DOF and weak in the pitching DOF, however, is no longer the driving frequency for the plunging DOF. At $U^* = 0.7$ the pitching and plunging modes have fully coalesced with a strong peak via self-interaction of the driving frequency, there are no longer superharmonics present. This form of limit cycle nonlinear frequency interaction remains for $U^* = 0.73$. Correlations can now be drawn between the state of the system and the strength of the quadratic nonlinearity. It is found that for reduced velocity values which coincide with linear/weakly nonlinear aerodynamics (that is, there exists a linear/weakly nonlinear relationship between the shock motion and the structure) the system exhibits very strong quadratic nonlinearity. However, as the strength of the aerodynamic nonlinearity increases, the coupling between the two types of nonlinearity (Type-B shock motion and freeplay) leads to a decrease in the strength of the quadratic interactions *i.e.* the system is no longer characterized by strong quadratic nonlinearity.

4 Conclusion

Higher-order statistics are utilized to provide new physical insights into the nonlinear aspects of a two-dimensional pitch/plunge airfoil system in transonic flow with a discontinuous concentrated structural nonlinearity. Bifurcation diagrams, phase plane plots and bicoherence contours are presented which provide new insight into how the nonlinear dynamic behavior of the system varies as the system evolves from aperiodic dynamic response to LCO and diverging flutter. By analyzing the behavior of the system at various reduced velocities the following insights are gained.

- The system shifts from aperiodic to limit cycle behavior as the reduced velocity increases.
- When the pitching and plunging modes are uncoupled, the system exhibits aperiodic behavior and a complex system of nonlinear interactions can be observed.
- As the pitching / plunging DOFs couple (with the plunging frequency in a super-harmonic ratio with the pitching frequency), the system moves to an ordered state with nonlinear interactions being limited to the driving frequency and its higher/lower harmonics.
- When the pitching/plunging frequencies coalesce, the system can be characterized by a periodic high-amplitude LCO and the nonlinear interactions occur predominantly via the coupled frequency self-interaction with slight indication of superharmonics.
- Quadratic nonlinearities are strongest when the freeplay nonlinearity is coupled with linear/weakly nonlinear aerodynamics.
- Strong nonlinear aerodynamics coupled with freeplay is characterized by a decrease in the strength of the quadratic nonlinearity whilst the cubic nonlinearity remains strong.

To complete this particular work, the tricoherence (cubic nonlinearity) should be taken into account and viscous effects included.

The characterization of nonlinear behavior presented in this study is an important step in the development of a nonlinear system identification framework for aircraft to be used for structural health monitoring purposes. Future development will include the extension of this type of analysis to three-dimensional wing and aircraft models investigating and characterizing various structural and inviscid/ viscous aerodynamic nonlinearities.

References

[1] Lee, B H K, Price S J, and Wong Y S, Non-linear aeroelastic analysis of airfoils: bifurcation and chaos. *Progress in Aerospace* Sciences, Vol. 35, No. 3, pp. 205–334, 1999.

[2] Vasconcellos R, Abdelkefi A, Hajj M R, and Marques F D, Grazing bifurcation in aeroelastic systems with freeplay nonlinearity. *Communications in Nonlinear Science and Numerical Simulation*, Vol. 19, No. 5, pp. 1611-1625, 2014.

[3] Kholodar D B, Nature of freeplay-induced aeroelastic oscillations. *Journal of Aircraft*, Vol. 51, No. 2, pp. 571-582, 2014.

[4] Kousen K A, and Bendiksen O O, Limit cycle phenomena in computational transonic aeroelasticity. *Journal of Aircraft*, Vol. 31, No. 6, pp. 1257-1263, 1994.

[5] Kim D H, and Lee I, Transonic and low-supersonic aeroelastic analysis of a two-degree-of freedom airfoil with a freeplay nonlinearity," *Journal of Sound and Vibration*, Vol. 234, No. 5, pp. 859-880, 2000.

[6] Dowell E H, Thomas H P, and Hall K C, Transonic limit cycle oscillation analysis using reduced order aerodynamic models. *Journal of Fluids and Structures*, Vol. 19, No. 1, pp. 17-27, 2004.

[7] Nikias C L, and Petropulu A P, *Higher-Order Spectra Analysis A Nonlinear Signal Processing Framework*, PTR Prentice-Hall, Inc., New Jersey, USA, 1993.

[8] Silva W A, Straganac T, and Muhamad R J, Higher-order spectral analysis of a nonlinear pitch and plunge apparatus. AIAA 2005-2013, 2005.

[9] Hajj M R, and Silva W A, Nonlinear flutter aspects of the flexible high-speed civil transport semispan model. *Journal of Aircraft* Vol. 41, No. 5, pp. 1202-1208, 2004.

[10] Silva W A, and Dunn S, Higher-order spectral analysis of f-18 flight flutter data. AIAA 2005-2014, 2005.

[11] Hajj M R, and Beran P S, Higher-order spectral analysis of limit cycle oscillations of fighter aircraft. *Journal of Aircraft*, Vol. 45, No. 6, pp. 1917-1923, 2008.

[12] Marzocca P, Nichols J M, Seaver M, Trickey S, and Milanese A, Second order spectra for quadratic non-linear systems by volterra functional series: analytical description and numerical simulation. *Mechanical Systems and Signal Processing*, Vol. 22, pp. 1882-1895, 2008.

[13] Candon M, Carrese R, Ogawa H, and Marzocca P, Identification and quantification of nonlinearities in a 2D aerofoil system with pitching and plunging freeplay nonlinearities via higher-order spectra. *7th Asia-Pacific International Symposium.*

[14] Candon M, Ogawa H, Carrese R, and Marzocca P, Identification of nonlinear aeroelastic behavior of a wing with pitching and plunging freeplay via higher--order spectra analysis. AIAA 2016-1953, 2016.

[15] Isogai K, On the transonic-dip mechanism of flutter of a sweptback wing. *AIAA Journal*, Vol. 17, No. 7, pp. 793-795, 1979.

[16] ANSYS® Academic Research, Release 16.2, Help System, Workbench Users Guide, ANSYS, Inc.
[17] Subba T, and Gabr M M, An Introduction to bispectral analysis and bilinear time series model, *Lecture Notes in Statistics*, Springer-Verlag 24, Berlin, 1984.
[18] Dalle Molle J W, and Hinich M J, The trispectrum. *Proceedings of the Workshop Higher Order Spectral Analysis*, Vail, pp.68-72, 1989.
[19] Pasquali, M., Lacarbonara, W., and Marzocca, P., Detection of nonlinearities in plates via higher-order-spectra: numerical and experimental studies. *Journal of Vibration and Acoustics*, Vol. 136, No. 4, pp. 1-13, 2014.
[20] Hickey D, Worden K, Platten M F, Wright J R, and Cooper J W, Higher-order spectra for identification of nonlinear modal coupling. *Mechanical Systems and Signal Processing*, Vol. 23, No. 4, pp.1037-1061, 2009.

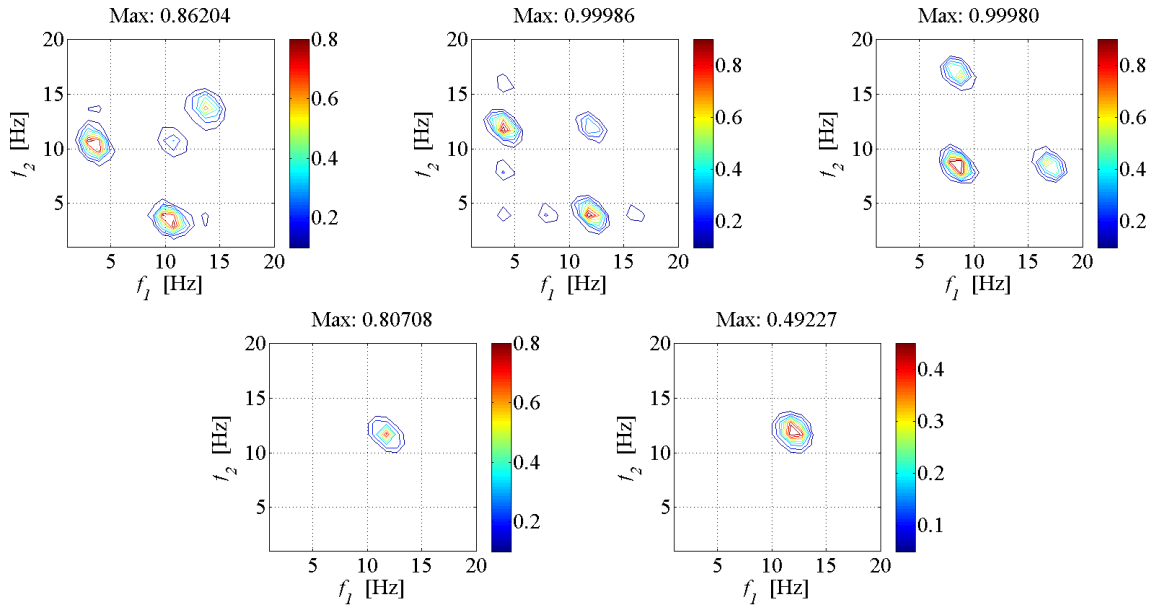

Figure 9: Bicoherence plots at the plunging DOF for *U = 0.3 (top left), *U** = 0.4 (top middle), *U** = 0.5 (top right), *U** = 0.7 (bottom left) and *U** = 0.73 (bottom right)**

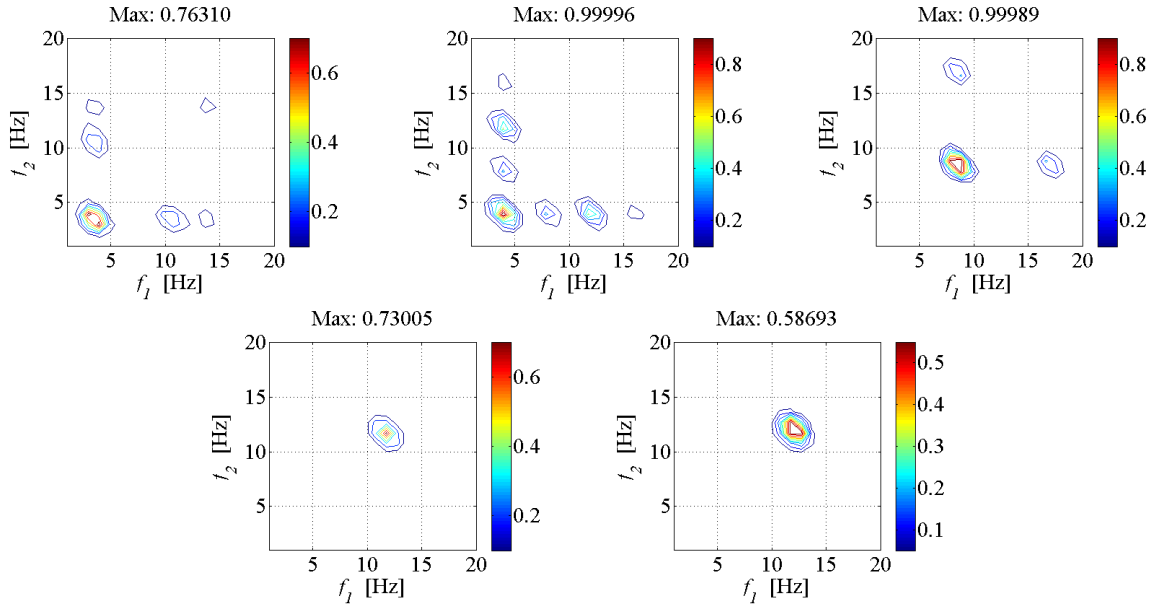

Figure 10: Bicoherence plots at the pitching DOF for *U = 0.3 (top left), *U** = 0.4 (top middle), *U** = 0.5 (top right), *U** = 0.7 (bottom left) and *U** = 0.73 (bottom right)**

Copyright Statement